

Potentiometric measurements of the spin-split subbands in a two-dimensional electron gas

P. R. Hammar and Mark Johnson
Naval Research Laboratory, Washington, DC 20375
 (Received 10 September 1999)

The density of states of carriers in a high-mobility InAs single quantum well is spin split by the Rashba effect. The asymmetry favors down-spin states for carriers with positive momentum and up-spin states for carriers with negative momentum. Imposing a bias current causes inequivalent shifts of the spin subband chemical potential, which are detected using a ferromagnetic film electrode and an open circuit voltage measurement. Measurements made on three samples over a range $77 < T < 296$ K demonstrate *spin detection* at a ferromagnet-semiconductor interface and corroborate earlier experimental results of spin-dependent interfacial resistance.

“Spin injection” in semiconductors has been a topic of interest for the past few decades, but there has been little experimental progress. Aronov proposed¹ that spin-polarized currents could be driven across a ferromagnet-semiconductor interface, with polarized carriers diffusing into the semiconductor for a finite distance. Later, following the successful demonstration of spin injection from a ferromagnet into a nonmagnetic metal,² Datta and Das proposed and discussed³ a gated two-dimensional electron gas (2DEG) device structure with ferromagnetic metal (FM) source and drain. The source-drain conductance is proportional to the relative orientation of the magnetization of the drain and the direction of the carrier spin. The latter is initially determined by the magnetization orientation of the source, but for certain orientations, the carrier spin (and hence the current polarization) precesses in a transverse effective magnetic field \mathbf{H}^* . The field \mathbf{H}^* derives from the Rashba effect⁴ and can be modified by the application of a gate voltage. Changing \mathbf{H}^* changes the spin precession rate and, therefore, the spin orientation at the FM drain, modulating the transconductance. Experimental attempts to fabricate this kind of structure and to demonstrate modulation of source-drain conductance have not succeeded.⁵ A recent theory proposed⁶ that spin injection at an FM/2DEG interface could be observed in a diode structure. The Rashba effect causes the spin subbands of the 2DEG to have different values of conductance, $g_{s,\uparrow} \neq g_{s,\downarrow}$, and a ferromagnetic electrode with proper magnetization orientation will measure spin-dependent current rectification: a fixed magnitude of current bias results in a voltage magnitude that differs for positive- or negative-polarity current in the 2DEG channel. A recent experimental observation of this effect⁷ provided a demonstration of spin injection at a FM/2DEG interface.

This paper introduces a model for understanding spin-dependent transport measurements in FM/2DEG structures and reports an additional set of experiments, using a different geometry, which support and confirm our earlier results.⁷ We begin with an examination of the effect of an imposed current on the Rashba spin splitting of the density of states of carriers in the 2DEG, and deduce the spin-dependent shifts of the chemical potential that vary according to the polarity of the bias. A FM film is then introduced in an open-circuit voltmeter geometry as a probe that is sensitive to the spin-up

(-down) chemical potential of the 2DEG carriers when the FM magnetization is oriented parallel (antiparallel) with the carrier spin-up axis. We have performed experiments in this “potentiometric” geometry on three of the same devices studied earlier, and the measurements correlate with those made in the “diode” geometry. The temperature dependence of the effect is discussed. We also report the results of experiments on a “control” sample, which conclusively demonstrate that fringe magnetic fields from the ferromagnetic electrode have no effect on our measurements.

According to the Rashba effect, spin-orbit coupling with an interfacial electric field arising from the asymmetry of the confining potential of the 2DEG adds a term to the Hamiltonian⁴

$$\mathcal{H}_{\text{SO}} = \alpha (\boldsymbol{\sigma} \times \mathbf{k}) \cdot \hat{\mathbf{z}}, \quad (1)$$

where $\boldsymbol{\sigma}$ are the Pauli spin matrices and $\hat{\mathbf{z}}$ is a unit vector normal to the plane of the 2DEG. The solution yields the electron energy dispersion relation for motion (with momentum $\hbar k_x$) in the 2DEG plane:

$$E(k) = \frac{\hbar^2 k_x^2}{2m^*} \pm \alpha k_x. \quad (2)$$

As plotted in Fig. 1(a), the carriers (with spin eigenstates along $\hat{\mathbf{y}}$) are degenerate at $k_x = 0$ and the spin splitting increases linearly with $|k_x|$. For $k_x > 0$ there are more carriers with spin down than with spin up, and the opposite is true for $k_x < 0$. This is depicted schematically by the density of states plot in Fig. 1(b), where the magnitude of the subband asymmetry $2\mu H^*$ (with μ the Bohr magneton) is of the order of a few meV and E_F , for our heterostructure, is about 250 meV.⁸ With zero bias current applied to a 2DEG channel [Fig. 1(c)], detailed balance requires that the number of electrons with $k_x > 0$ equal the number with $k_x < 0$, and the number of up-spin carriers equal the number of down-spin carriers.

The situation changes for nonzero bias current. The Fermi sea is a paraboloid of revolution about the E axis, and the resulting Fermi surface is the pair of concentric circles shown as the solid lines in Fig. 2(a), with radii $k_{F,\text{max}}$ and $k_{F,\text{min}}$, and with the spin orientation denoted by arrows. Imposition of a positive current displaces the Fermi sea (and circles) to the right by δk [dotted lines of Fig. 2(a)]. For the

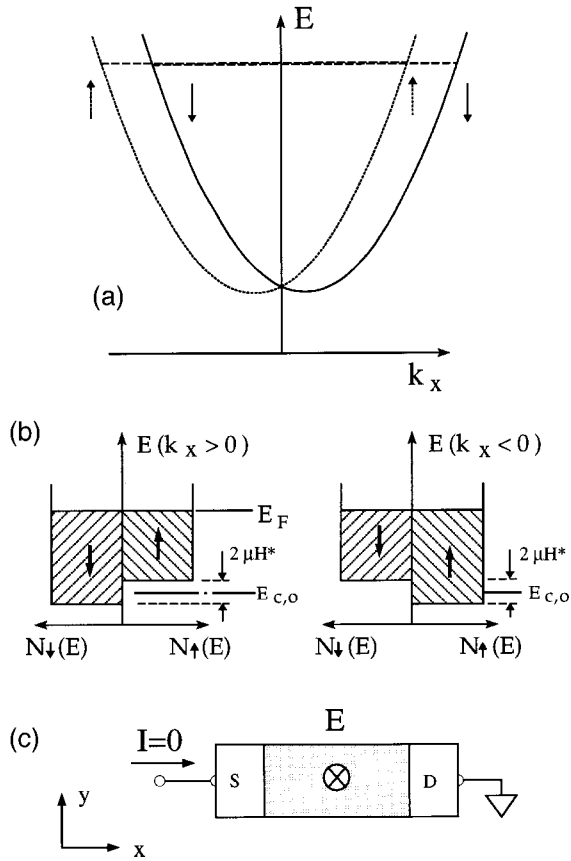


FIG. 1. (a) For 2DEG carriers, E vs k showing spin splitting. (b) Density of states for $k_x > 0$ and for $k_x < 0$. (c) Schematic top view of a 2DEG channel spin structure, showing directions of the bias current I and the electric field \mathbf{E} arising from the asymmetric confining potential.

branch $k_x > 0$, up-spin carriers are added at $k_{F,\min}$ and down-spin carriers at $k_{F,\max}$. The chemical potentials of both the up-spin and down-spin subbands are raised, but the chemical potential of the down-spin subband is raised more than that of the up-spin subband because the area of added states near $k_{F,\max}$ is larger than that at $k_{F,\min}$. Similarly, for the branch $k_x < 0$, up-spin carriers are depleted at $k_{F,\min}$ and down-spin carriers are depleted at $k_{F,\max}$. The resulting densities of states for both $k_x > 0$ and $k_x < 0$ are sketched in Fig. 2(b). For the imposition of a negative-bias current, the Fermi circles are shifted to the left by $-\delta k$, and the resulting shifts of chemical potential for both $k_x > 0$ and $k_x < 0$ are depicted in Fig. 2(c).

These relative shifts of the spin subband chemical potential can be measured by using the FM thin-film electrode F in the potentiometric geometry of Fig. 3(a). Here F is connected to an infinite-impedance voltmeter and an external magnetic field is applied along the \hat{y} axis. As seen schematically with the simple band picture of Fig. 3(b), when the magnetization is along $-\hat{y} + \hat{y}$ the chemical potential of the ferromagnet $N(E_F)$ is essentially the same as that of the ferromagnet up-spin [down-spin] subband, $N_\uparrow(E_F)$ [$N_\downarrow(E_F)$], and it aligns with the up-spin [down-spin] subband chemical potential of carriers in the 2DEG.² Changing the magnetization between orientations along $\pm \hat{y}$ therefore measures the spin subband difference of chemical po-

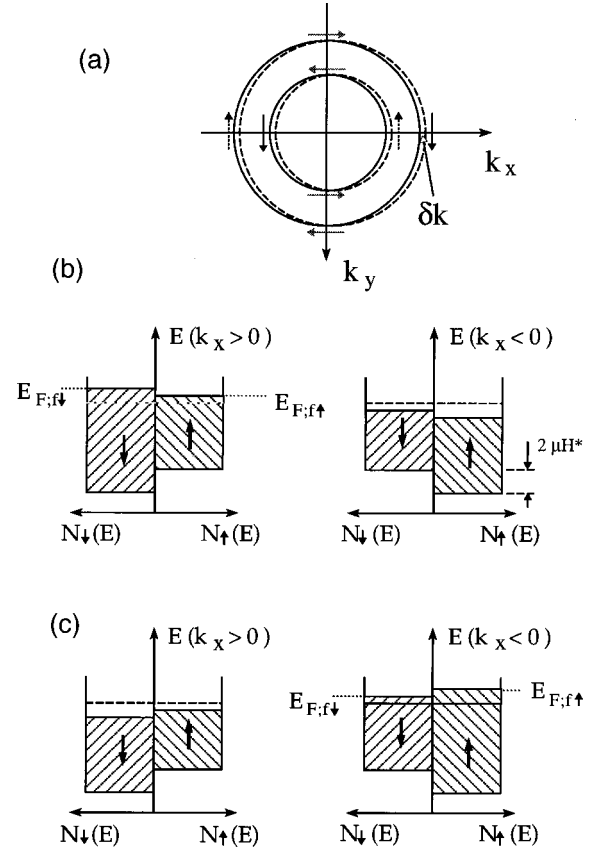


FIG. 2. (a) Fermi surface (concentric circles, solid lines), including the case for a shift of $+\delta k_x$ (dotted lines) resulting from the imposition of a bias current. (b) Density of states DOS for positive-bias current. (c) DOS for negative-bias current. Note the shifts of the chemical potential of the spin subbands.

tential in the 2DEG with an accuracy of η , where $\eta \approx [N_\uparrow(E_F) - N_\downarrow(E_F)] / \frac{1}{2}[N_\uparrow(E_F) + N_\downarrow(E_F)]$ is the polarization of carriers near E_F in the ferromagnet. We note from Figs. 2(b) and 2(c) that the symmetry of the measurement will be reversed when the polarity of the bias current in the 2DEG is reversed. A detailed theory and calculation of the magnitude of these shifts of chemical potential are beyond

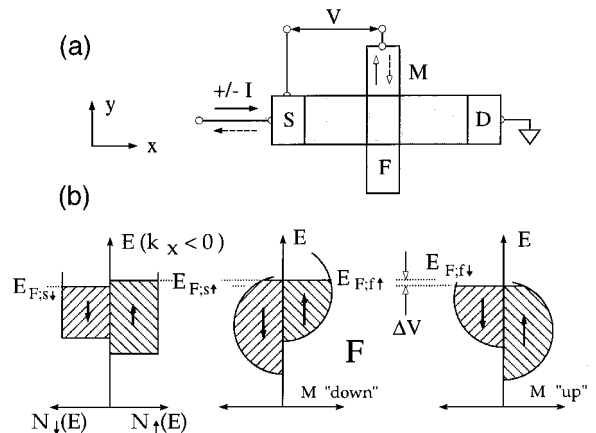


FIG. 3. (a) Schematic top view of the potentiometric geometry. (b) DOS diagrams showing how the chemical potential of the FM aligns with the spin subband chemical potentials of the 2DEG.

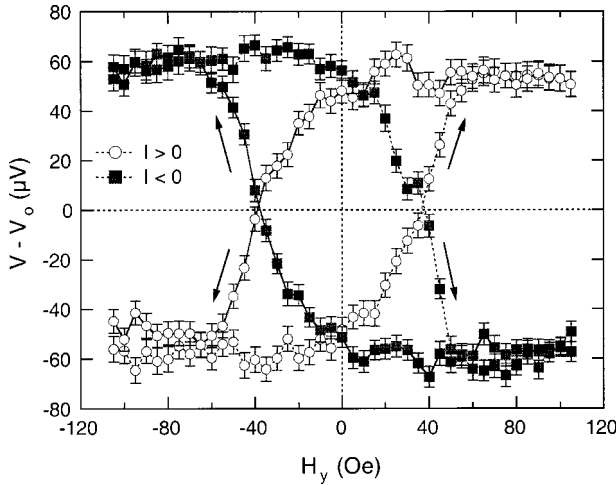


FIG. 4. Potentiometric measurements on sample BB-A1 at $T = 77$ K, for positive- (circles) and negative- (squares) bias current and for field sweeps along $\pm \hat{y}$.

the scope of this paper. Here we report experimental data in qualitative support of this model and in quantitative agreement with our earlier results.

Several of the samples that were measured in the diode configuration⁷ were wired in the potentiometric geometry of Fig. 3(a), and measurements V were recorded for both current polarities, for magnetic field sweeps along $\pm \hat{y}$ sufficiently large to reverse the magnetization of the FM film, for a variable current magnitude in the range $0.05 < I < 1.0$ mA and over the temperature range $50 < T < 295$ K. An example of the data is shown in Fig. 4 for a typical sample, sample BB-A1, at $T = 77$ K and $I = \pm 100$ μ A. Arrows indicate the direction of the field sweep, and the hysteresis corresponds to the hysteresis of $M(H_y)$ of F .⁷ The base line voltage of 26.0 mV (-25.7 mV) representing the voltage drop between F and the ground of the voltmeter [refer to Fig. 3(a)] has been subtracted. The symmetry of the $V(H_y)$ loop is reversed when the polarity of the bias current is reversed, as predicted by the above model. The voltage difference $\Delta V = |V(H_y > 50 \text{ Oe}) - V(H_y < -50 \text{ Oe})| = 110$ μ V represents a measure of the difference of spin subband chemical potential in the 2DEG induced by the Rashba effect. It is linear with current for the experimental range and is discussed below as $\Delta R_p = \Delta V/I$. We note that ΔR_p has the same dependence on field angle θ , $\Delta R_p(\theta) \propto \cos(\theta)$ (with $\theta = 0$ along \hat{y}), as the diode measurements $\Delta R_i(\theta)$,⁷ consistent with theory.⁶

Values of ΔR_p measured on sample BB-A1 in the potentiometric geometry are compared with values ΔR_i measured in the diode geometry in Fig. 5 over the temperature range $50 < T < 295$ K. For the range $100 < T < 295$ K, the values of the spin-dependent resistance change are the same within experimental error, $\Delta R_i = \Delta R_p$. Below $T = 100$ K, the magnitude of ΔR_i (squares) levels off, but that of ΔR_p (circles) continues to increase until $T = 70$ K where it, too, ceases to vary with temperature. The correspondence in values between roughly $77 < T < 296$ K confirms that the changes in interface conductance measured in the diode geometry⁷ are closely related to the shifts of the subband chemical potential that result from the bias-current-induced asymmetries in the spin-split carrier distributions of the 2DEG. Reasons for the divergence below $T = 100$ K may become clear when a more

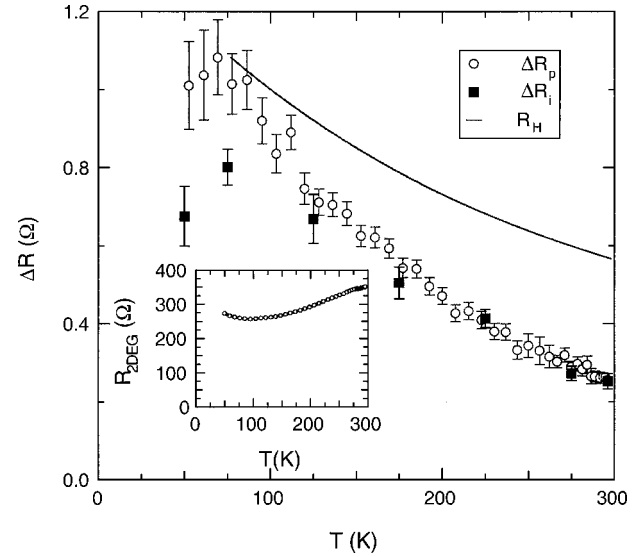


FIG. 5. (a) ΔR_p and ΔR_i vs T on sample BB-A1. Both measurement geometries show the same spin-dependent resistance change for $100 < T < 296$ K. The Hall coefficient $R_H(T)$ is normalized to match the same scale as ΔR_p .

complete theory has been developed. Although it is not surprising that ΔR_i and ΔR_p decrease with increasing temperature, a detailed explanation of the temperature dependence is not yet known. Possible mechanisms might include thermal smearing of the spin subband populations, dilution by leakage currents (or hole currents) that are spin randomized during conductance across the interface, or temperature dependence of the confining potential, which is the source of the Rashba splitting.

Finally, to examine the plausibility that fringe magnetic fields near the FM might generate spurious Hall voltages in our samples, we performed two ‘‘control’’ experiments. First, the Hall coefficient R_H was measured, after sample fabrication, on a cross region of sample BB-A1 about 0.3 μ m from the edge of the FM film. External fields up to $|H_z| = 130$ Oe were applied perpendicular to the plane of the 2DEG at several temperatures in the range $77 < T < 296$ K. Plotted in Fig. 5 on a scale equivalent with ΔR_p , $R_H(T)$ decreases by a factor of 1.9 as temperature is increased from $T = 77$ to 296 K. By contrast, ΔR_p decreases by a factor of 4.2 over the same temperature range. These temperature dependences are distinctly different. Since any fringe field Hall effect must have the same temperature dependence as $R_H(T)$, we conclude that no such effect contributes to our observed voltages.

Second, on the same chip as the other devices, we fabricated a device designed to have a fringe field Hall effect. For this device, the ‘‘source’’ region [refer to Fig. 3(a)] was fabricated as a Hall cross with dimensions of a few μ m, the potentiometric measurement was referenced to one of the vertical arms of the cross, and the FM film overlapped the edge of the cross region by about 0.5 μ m. For field sweeps along the \hat{x} axis, a hysteretic voltage $V(H_x)$ was recorded for the potentiometric configuration. This is expected for such a device⁹ because fringe fields at the edge of the FM film generate Hall voltages in the 2DEG cross included in the potentiometric circuit. The temperature dependence was the same as $R_H(T)$ in Fig. 5 for our two experimental tempera-

tures, $T=77$ and 296 K, confirming that the fringe field Hall effects have the same temperature dependence as R_H . However, measurements in the “diode geometry” (which did not involve a vertical arm of the “source” Hall cross) failed to show any voltage $V(H_x)$, even though potentiometric measurements demonstrate that fringe fields must exist. This is because the FM electrode has a low resistance and voltages that would be developed across the width of the channel (along \hat{y}) cannot be sustained along the low impedance of the FM film. We conclude that our geometry strongly inhibits the development of spurious voltages and that any such voltages would be readily identified by their temperature dependence.

In summary, we have introduced a steady-state Fermi surface model for understanding spin-dependent transport measurements in FM/2DEG structures. This model is valid for diffusive transport and elevated temperatures. We have made

measurements in a “potentiometric” geometry on three of the same samples that were measured in the “diode” geometry. For the temperature range $77 < T < 296$ K, the magnitudes ΔR_p and ΔR_i for the two geometries were the same, within experimental error. At lower temperatures, these values differ, with ΔR_p being about 30%–40% larger. We also performed “control” experiments that eliminate the possibility that fringe field Hall effects might contribute to our measured voltages.

This work was supported by the Office of Naval Research and the Defense Advanced Research Project Agency. P.R.H. was supported by the National Research Council. M.J. gratefully acknowledges the partial support of ONR Grant No. N000-1499-AF0002. The authors gratefully acknowledge stimulating conversations with R. H. Silsbee and M. J. Yang and thank B. R. Bennett for supplying the III-V heterostructures.

¹A. G. Aronov and G. E. Pikus, *Fiz. Tekh. Poluprovodn.* **10**, 1177 (1976) [*Sov. Phys. Semicond.* **10**, 698 (1976)].

²Mark Johnson and R. H. Silsbee, *Phys. Rev. Lett.* **55**, 1790 (1985); *Phys. Rev. B* **37**, 5312 (1988); **37**, 5326 (1988).

³S. Datta and B. Das, *Appl. Phys. Lett.* **56**, 665 (1990).

⁴Y. A. Bychkov and E. I. Rashba, *Pis'ma Zh. Eksp. Teor. Fiz.* **39**, 66 (1984) [*JETP Lett.* **39**, 78 (1984)].

⁵A. Filipe, A. Schuhl, and P. Galtier, *Appl. Phys. Lett.* **70**, 129 (1997); M. Zölfl *et al.*, *J. Magn. Magn. Mater.* **175**, 16 (1997); A. Cabbibo *et al.*, *J. Vac. Sci. Technol. A* **15**, 1215 (1997); B. T.

Jonker, O. J. Glembocki, R. T. Holm, and R. T. Wagner, *Phys. Rev. Lett.* **79**, 4886 (1997).

⁶Mark Johnson, *Phys. Rev. B* **58**, 9635 (1998).

⁷P. R. Hammar, B. R. Bennett, M. J. Yang, and Mark Johnson, *Phys. Rev. Lett.* **83**, 203 (1999).

⁸For an explanation of the self-consistent confining potential calculation, see Fu-Cheng Wang, W. E. Zhang, C. H. Yang, M. J. Yang, and B. R. Bennett, *Appl. Phys. Lett.* **69**, 1417 (1996).

⁹Mark Johnson, B. R. Bennett, M. J. Yang, M. M. Miller, and B. V. Shanabrook, *Appl. Phys. Lett.* **71**, 974 (1997).